

## *Echium angustifolium* Reduces/Revokes the Effect of *Cerastes cerastes* Venom in Albino Mice

Inass A Sadawe<sup>1</sup>, Nisreen H Meiqal<sup>1</sup>, Amira A Gbaj<sup>2</sup>, Salah M Bensaber<sup>1</sup>, Abdulathim A A Alshoushan<sup>3</sup>, Halima A Gbaj<sup>1</sup>, Jamal A Elbakay<sup>1</sup>, Massaud Salem Maamar<sup>4</sup>, Anton Hermann<sup>5</sup> and Abdul M Gbaj<sup>1\*</sup>

<sup>1</sup>Department of Medicinal Chemistry, Faculty of Pharmacy, University of Tripoli, Libya

<sup>2</sup>Novelien School, Tripoli Centre, Tripoli, Libya

<sup>3</sup>Food and Drug Control Centre (LFDA), Tripoli, Libya

<sup>4</sup>Zoology Department, Faculty of Science, Tripoli University, Libya

<sup>5</sup>Department of Biosciences, University of Salzburg, Salzburg, Austria

**\*Corresponding Author:** Abdul M Gbaj, Professor of Genetics and Biochemistry, Department of Medicinal Chemistry, Faculty of Pharmacy, University of Tripoli, Libya.

**Received:** September 11, 2020; **Published:** September 28, 2020

### Abstract

Snakebites are a tremendous challenge in public health owing to their high mortality. Most snake venoms cause powerful local tissue damage leading to transitional or permanent disability of victims. The anti-*Cerastes cerastes* venom effect of aqueous aerial parts of *Echium angustifolium* extract was explored using molecular modelling and animal models. The improvement in the mean survival time of albino mice was used to construe the antivenom property of this extract after challenging with LD99 snake venom. *Echium angustifolium* aqueous extract constituents (pyrrolizidine alkaloids, phenolic acid derivatives and flavonoids) showed *van der Waals*, hydrogen bonding and electrostatic interactions with an active site of the main constituents of the venom phospholipases A<sub>2</sub> enzyme and changes in the fluorescent spectrum of the enzyme. The aqueous extract of *Echium angustifolium* extract applied intraperitoneally considerably increased the mean survival time but could not protect animals from death when used alone. The lower dose of 0.5 ml *Echium angustifolium* extract (1.29g/30 ml) showed less protective activity of 8.5 hours in comparison to the higher dose 2.0 ml (1.29g/30 ml) which gave a 13 hour protection time. The anti-snake venom was found to be more efficient than the aqueous aerial parts of *Echium angustifolium* extract.

**Keywords:** *Cerastes cerastes*; Anti-Snake Venom; Aqueous *Echium angustifolium*; Molecular Modelling/Modelling

### Introduction

Snakebites signify a considerable public health threat that leads to high morbidity and mortality in many states of North Africa including Libya, Tunisia, Algeria and Egypt [1,2]. More than four hundred snake species, of which about thirty are venomous, belong to 4 terrestrial dissimilar families mainly: *Atractaspididae*, *Colubridae*, *Viperidae* and *Elapidae* are responsible for a majority of human fatalities, as stated by the World Health Organization (WHO) [3]. *Cerastes cerastes* is solitary of the prominent snakes related to human mortality in Libya, Tunisia and Algeria. The *Cerastes cerastes* venom contains a variety enzymes including proteolytic compounds and causes multiple kinds of intoxications [4]. The resulting toxicities, lead to considerable physiopathological changes of the skin, liver and heart. Phospholipase A<sub>2</sub> (PLA<sub>2</sub>) for instance, has been shown to be connected with several toxicities such as lung-, neuro-, nephro-, cardio-, and

hepatotoxicity [5-7]. The lethal effect of snake venom mainly results from PLA<sub>2</sub>. Phospholipid hydrolysis by PLA<sub>2</sub> liberates an important acid called arachidonic acid whose metabolism leads to the formation of lipid peroxides and highly toxic reactive oxygen species (ROS) [7,8]. The increased activity of liver enzymes is an indicator of liver injuries as well other organs [7,9]. The neurotoxic effects exerted by PLA<sub>2</sub> appear to be due to the influx of calcium ions *via* voltage-gated ion channels located in the neuronal membrane [7,9]. In addition, PLA<sub>2</sub> affects mitochondrial membranes in respiratory muscles due to phospholipid hydrolysis. These two effects together lead to acute neuromuscular weakness and eventually to paralysis and suffocation [10,11].

Anti-snake venom (ASV) is a major antidote choice for snake venom actions and the basis of treatment. Monovalent ASV (a hyperimmunizing venom that is obtained from a single species of snake) is favored to the polyvalent venom (obtained from various snake species) since it is less perilous to the patient and probably more effective in the neutralization of the specific venom though, a species diagnosis has to be made before the proper treatment can be selected. Polyvalent ASV is frequently used against snakebite, but it is more costly since antibodies are from several immunized animals. This in turn can cause adverse reactions due to activation of the immune system in patients [12,13].

*Echium angustifolium* (family: *Boraginaceae*), a wildflower is growing in Mediterranean regions such as Libya, Algeria, Tunisia, Greek, etc. The plant contains Allantoin and pyrrolizidine alkaloids (i.e. Heliosupin), phenolic acid derivatives, flavonoids and other constituents which are known for their numerous biological activities. It is weakly poisonous for small warm-blooded animals but not dangerous for humans and sheep even neutralize the active ingredients in their stomach. In small doses this medical plant is used as diuretic, anti-inflammatory, astringent or antirheumatic. However, after prolonged ingestion it may cause liver damage or will be carcinogenic [14,15]. In the present study an aqueous extract of *Echium angustifolium* was investigated for its ability to reduce or revoke the effect of *Cerastes cerastes* crude venom in mice.

Molecular docking and *in vivo* animal studies were performed in order to determine the prospective effect of the plant extract to *Cerastes cerastes* venom. Molecular docking results provide information that can be used to direct and extend an array of experiments [16,17]. Among the molecules that were evaluated using molecular modelling against *Cerastes cerastes* PLA<sub>2</sub> hesperidin and naringenin were the most potent. The aim of our study was to screen the potential anti-snake venom potential of *Echium angustifolium* aerial part constituents compared to polyvalent ASV using molecular modelling and albino mice models. Our results revealed that *Echium angustifolium* constituents form hydrogen bonds with active sites of PLA<sub>2</sub> which reduces or revokes the effect of *Cerastes cerastes* venom.

## Materials and Methods

### Collection of plant material and preparation of aqueous extracts

Plants were collected from the Garabolle Zone, Tripoli, Libya (March 2020), and *Echium angustifolium* was identified and authenticated by a botanist. The sample was rinsed with deionised water and dried at classical room temperature. The leaves with the stems were cut into smaller pieces and 1.29g of the sample was taken. The cut leaves and stems were then grinded in a homogenizer (HO4A Edmund Buhler GmbH, UK) along with 30 ml of distilled water. The resulting aqueous solution was filtered under vacuum using a Millipore filter (0.45 µm, GHD Acrodisc GF, UK) and the filtrate was stored at 4°C.

### Snake venoms

To assure its freshness/purity, *Cerastes cerastes* snake crude venoms were obtained by causing snake bit through a parafilm-coated container to eject venom. Snakes are reared at the Zoology Department, Faculty of Science, Tripoli University (Libya) and the extracted venom was stored at -20°C until use. An aliquot of 7.5 µl from the ejected venoms was added to 800 µl of normal saline (0.9% NaCl). A dose of 100 µl (100 ng) was given intraperitoneally to the Swiss albino mice.

### Molecular docking

The starting geometry of the *Echium angustifolium* constituents was constructed using chem3D Ultra (version 8.0, Cambridge soft Com., USA). The optimized geometry of *Echium angustifolium* constituents with the lowest energy was used for molecular docking studies. Crystal structures of cobra-venom PLA<sub>2</sub> in a complex with a transition-state analogue (1POB) was obtained from the PDB (Protein Data Bank) <https://www.rcsb.org/structure/1POB>. Molecular dockings of *Echium angustifolium* constituents with 1POB was accomplished by Auto Dock 4.2 software from the Scripps Research Institute (TSRI) (<http://autodock.scripps.edu/>). Firstly, polar hydrogen atoms were added into protein molecules. Then, partial atomic charges of the PLA<sub>2</sub> enzymes and *Echium angustifolium* constituents were calculated using Kollman methods [18]. In the process of molecular docking, the grid maps of dimensions (62Å X 62Å X 62Å) with a grid-point spacing of 0.376Å and the grid boxes centered. The number of genetic algorithm runs and the number of assessments were set to 100. All other parameters were default settings. Cluster analysis was performed on docking results by using a root mean square (RMS) tolerance of 2.0Å, which was reliant on the free energy binding ability. Lastly, the dominating configuration of the binding complex of *Echium angustifolium* constituents and PLA<sub>2</sub> enzyme fragments with minimum binding energy were determined which depended potentially on the data of 3D structures of the PLA<sub>2</sub> binding sites and finally produced a succession of phospholipase binding complexes.

### Absorbance spectra

Absorbance spectra were measured on a Jenway model 6505 UV-visible spectrophotometer, (London, UK) using quartz cells of one centimeter path length. UV-Vis absorbance spectra were measured in the 200-500 nanometer range, spectral bandwidth of three-nanometer. For the final spectrum of each solution analyzed baseline subtraction of the buffer solution was performed. The venoms samples protein content of was obtained by the spectrophotometric method of Markwell, *et al* [19]. BSA (Bovine serum albumin, Sigma) was used for standard assays.

### Fluorescence spectra

Fluorescence emission and excitation spectra were measured using a Jasco FP-6200 spectrofluorometer (Tokyo, Japan) using fluorescence 4-sided quartz cuvettes of 1.00 cm path length. The automatic shutter-on function was used to minimize photo bleaching of the sample. The selected wavelength was utilized to provide combined excitation of tyrosine and tryptophan residues. The buffer emission spectrum was subtracted from the full emission spectrum to omit the background fluorescence. The changes of fluorescence emission strength and fluorescence shifts were observed in which the formation of the system was formed by sequential addition of aliquots of Tris buffer, *Cerastes cerastes* venom and finally *Echium angustifolium* filtered aqueous extract.

### Test animals

Swiss albino male mice (18 ± 2g) were used for *in vivo* experiments. In order to diminish the contact caused by handling and environmental alterations during behavioral studies, mice were adapted to laboratory surroundings and the Laboratory Animal Holding Center for three days and the laboratory room as a minimum two hour prior to experimentation, respectively. Animals were kept under standard conditions with food (low protein diet) and water available *ad libitum*. The animals were housed six per cage in a light-controlled room (12h light/dark cycle, light on 07:00h) at 65% relative humidity and 27°C. All experiments were performed between 10:30 and 15:00h. Each test group consisted of at least six mice, and each mouse was used only once. All animal experiments were conducted according to guidelines set by the Institutional Animal Ethics Committee of the Tripoli University.

### Detoxification of venom by *Echium angustifolium* extract

Five groups (six mice each) were used in this study. The first group received only 100 µl (100 ng of total protein) of the *Cerastes cerastes* venom (LD<sub>99</sub>, 5 µg/kg). Groups 2 - 4 (serving as treatment groups) were given an equal quantity of the *Cerastes cerastes* venom with 0.5

ml, 1.0 ml and 2.0 ml of aqueous *Echium angustifolium* extract orally (1.9g/30 ml). Group 5 received 100 µl of the *Cerastes cerastes* venom and ASV. The number of deaths was recorded within 24h.

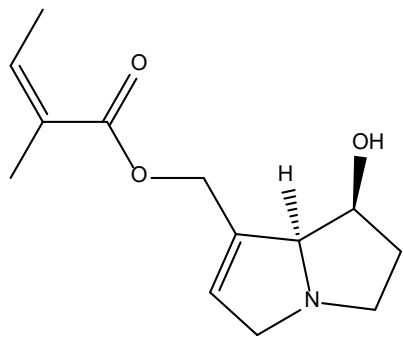
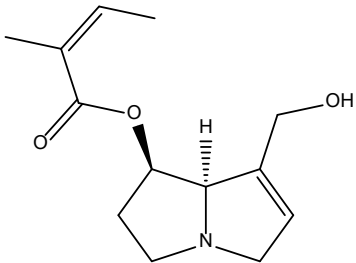
**Statistical analysis**

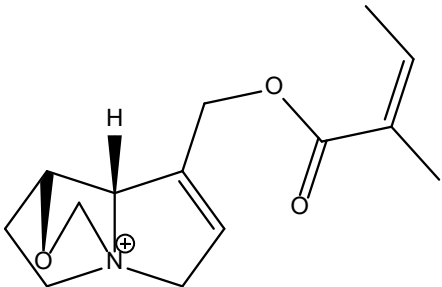
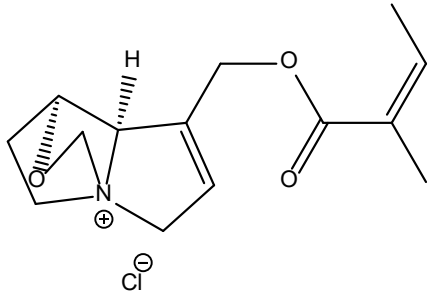
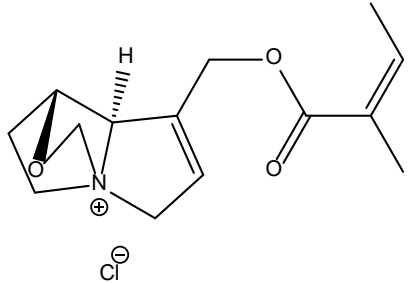
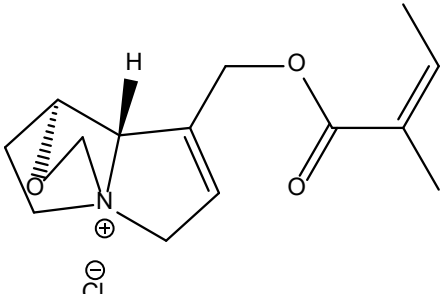
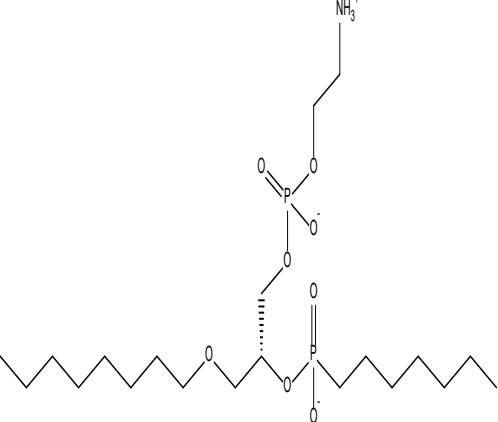
The significance of difference among the various treated groups and control group were analyzed by means of one-way ANNOVA using unpaired student’s *t* test. The results were expressed as the mean ±SEM of the number of experiments performed, with P < 0.05 indicating significance.

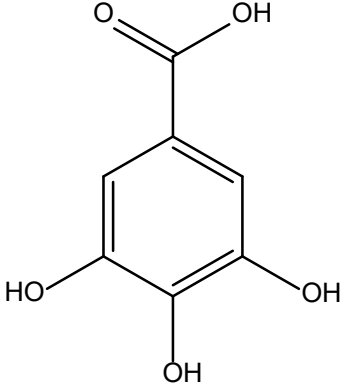
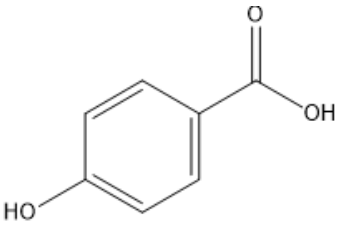
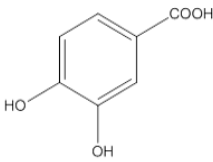
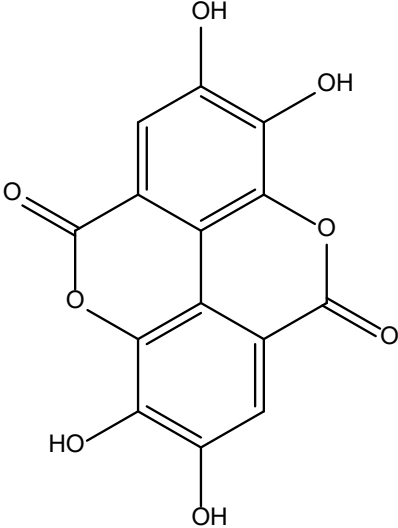
**Results and Discussion**

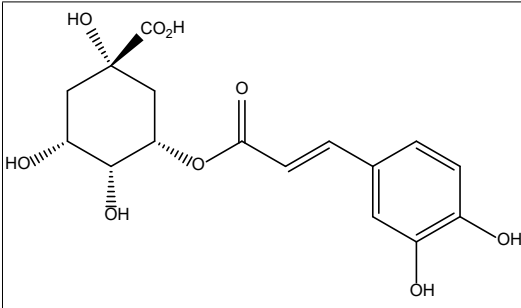
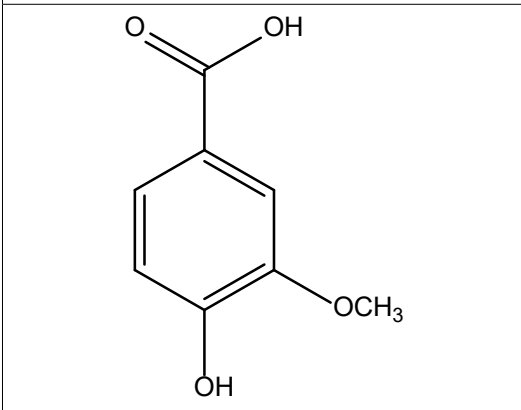
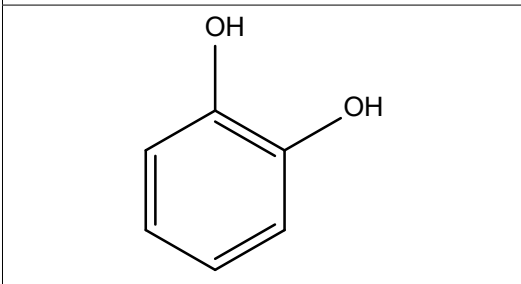
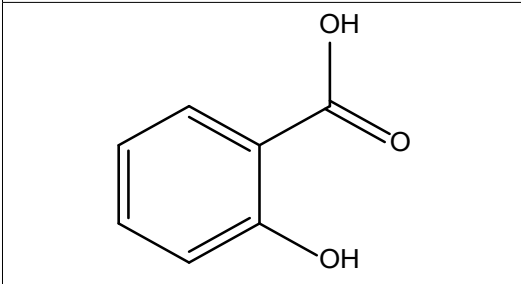
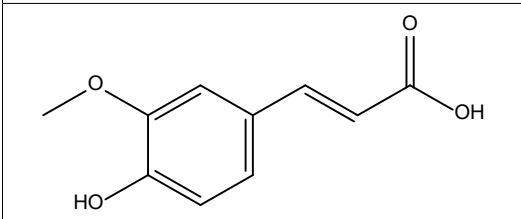
**Molecular docking analysis**

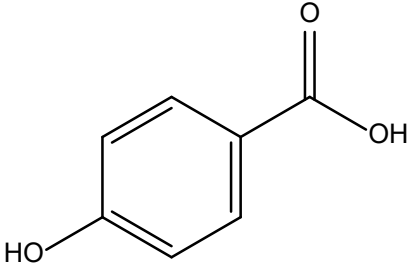
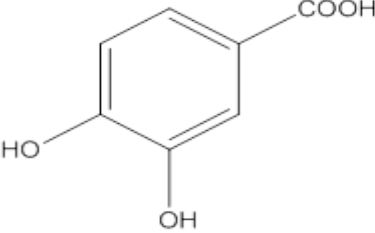
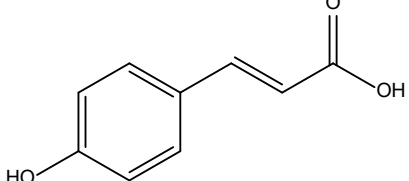
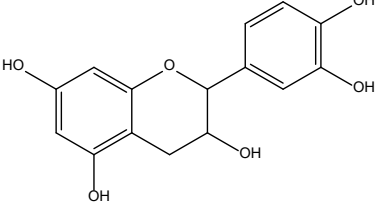
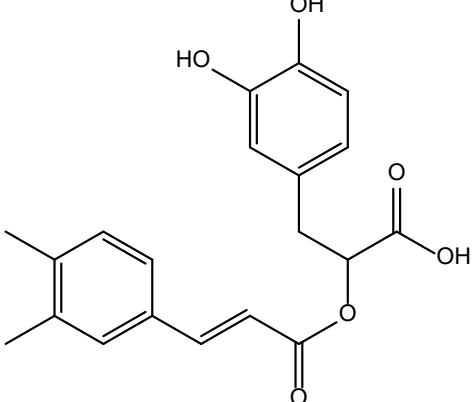
Table 1 shows the binding energies of *Echium angustifolium* constituents and cobra-venom PLA<sub>2</sub> (1pob) obtained by the molecular docking strategy. In this study, molecular dockings of the *Echium angustifolium* constituents with cobra-venom phospholipase A<sub>2</sub> (1pob) were performed using Auto Dock 4.2 to investigate the binding mode of *Echium angustifolium* constituents with cobra-venom phospholipase A<sub>2</sub> (1pob) and to obtain information about interaction forces between *Echium angustifolium* constituents and cobra-venom phospholipase A<sub>2</sub> (1pob). *Echium angustifolium* constituents and cobra-venom PLA<sub>2</sub> (1pob) were kept as flexible molecules and were docked into seven forms of rigid PLA<sub>2</sub> to obtain the preferential binding site to *Echium angustifolium* constituents on phospholipase A<sub>2</sub>. The molecular docking results are shown in table 1. The modeling studies showed that there are *van der Waals*, hydrogen bonding and electrostatic interactions between *Echium angustifolium* constituents with PLA<sub>2</sub>. The contribution of *van der Waals* and hydrogen bonding interaction is much greater than that of the electrostatic interaction because the sum of *van der Waals* energy, hydrogen bonding energy and desolvation free energy is larger than the electrostatic energy, which is consistent with the literature [20,21]. Hesperidin and cobra-venom PLA<sub>2</sub> (1pob) interactions are shown in figure 1. Hesperidin showed a higher binding energy (-9.60 kcal/mol,) compared to standard Gel (-4.26 kcal/mol) as mentioned in table 1. Figure 1 shows seven hydrogen bonds between hesperidin and cobra-venom PLA<sub>2</sub> while Gel shows six hydrogen bonds with cobra-venom phospholipase A<sub>2</sub> (data not shown). In addition, hesperidin showed good docking interaction with the cobra-venom PLA<sub>2</sub> binding site (GLY29, ASN52, TYR63and GLU55) (Figure 1). The interaction of *Echium angustifolium* constituents with the cobra-venom PLA<sub>2</sub> binding site of the enzyme is essential for effective inhibition as previously reported for Gel and other polyphenols [22,23]. Therefore, *Echium angustifolium* constituents and Gel may be considered as effective PLA<sub>2</sub> inhibitor.

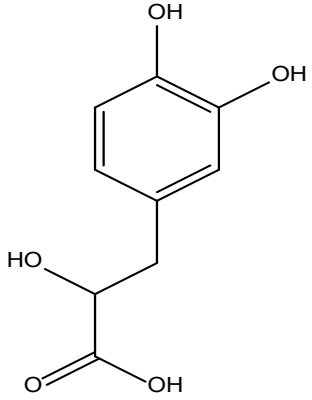
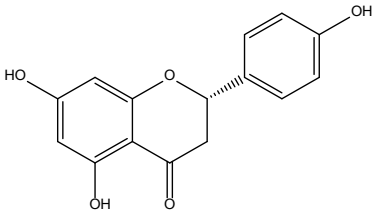
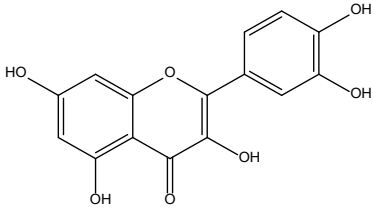
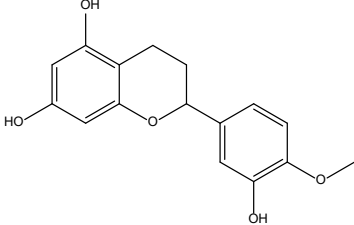
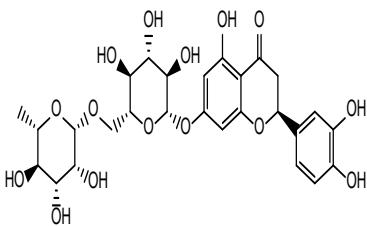
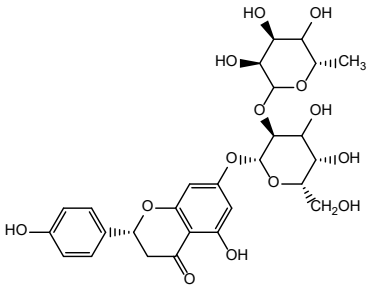
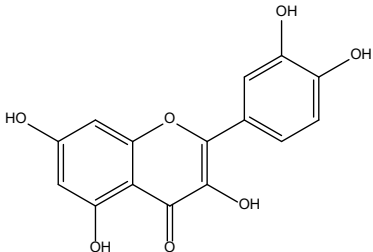
Chemical structures	Chemical nature	Name of ligand	1Pob Binding energy
	Pyrrolizidine Alkaloids	9-angeloylretronecine	-6.3
	Pyrrolizidine Alkaloids	7-angeloylretronecine	-6.6

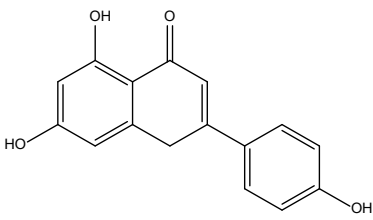
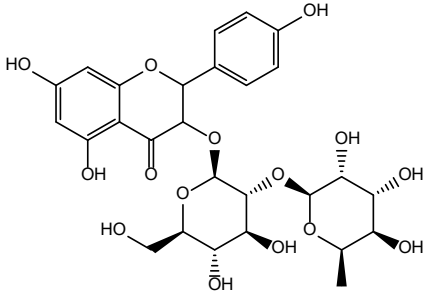
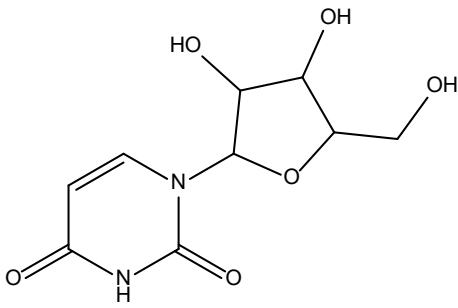
	Pyrrolizidine Alkaloids	(7 <i>R</i> , 8 <i>S</i> )-petranine 3	-7.0
	Pyrrolizidine Alkaloids	(7 <i>S</i> , 8 <i>R</i> )-petranine 1	-6.9
	Pyrrolizidine Alkaloids	(7 <i>R</i> , 8 <i>R</i> )-petranine 4	-7.1
	Pyrrolizidine Alkaloids	(7 <i>R</i> , 8 <i>S</i> )-petranine 2	-7.1
	1-O-Octyl-2-Hep-tylphosphonyl-SN-Glycero-3-Phosphoethanolamine	Gel	-4.26

	Phenolic acid derivatives	Gallic acid	-6.0
	Phenolic acid derivatives	Benzoic acid	-5.9
	Phenolic acid derivatives	Protocatechuic acid	-5.8
	Phenolic acid derivatives	Ellagic acid	-8.6

	Phenolic acid derivatives	Chlorogenic acid	-8.5
	Phenolic acid derivatives	Vanillic acid	-6.0
	Phenolic acid derivatives	Catechol	-5.3
	Phenolic acid derivatives	Salicylic acid	-6.2
	Phenolic acid derivatives	Ferulic acid	-6.5

 <p>p-hydroxy benzoic acid</p>	Phenolic acid derivatives	p- hydroxy- benzoic acid	-5.9
 <p>(12) protocatechuic acid</p>	Phenolic acid derivatives	Protocatechuic acid	-5.8
	Phenolic acid derivatives	P-Coumaric acid	-6.4
	Phenolic acid derivatives	Catechin	-8.3
	Phenolic acid derivatives	Rosmarinic acid	-8.6

	Phenolic acid derivatives	Dihydroxyphenyl lactic acid	-6.6
	Flavonoid	Naringin	-8.4
	Flavonoid	Rutin	-8.1
	Flavonoid	Hesperetin	-8.1
	Flavonoid	Hesperidin	-9.6
	Flavonoid	Naringenin	-9
	Flavonoid	Quercetin	-8.4

	Flavonoid	Apigenin	-8.1
	Flavonoid	Kaempferol-3-neohesperidoside	-8.6
	pyrimidine-analog	Uridine	-6.6

**Table 1:** Binding energies of *Echium angustifolium* constituents and cobra-venom phospholipase A<sub>2</sub> (1pob) obtained from molecular docking studies. The unit of all energies ( $\Delta G$ ) is kcal/mol.

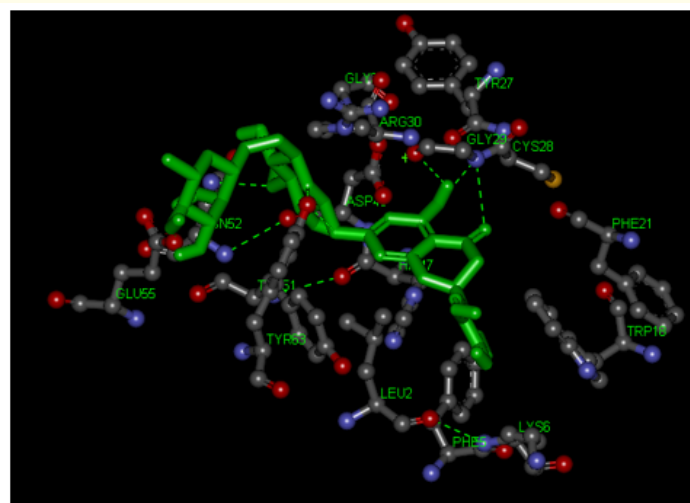


**Figure 1:** Interaction model of hesperidin and cobra-venom PLA<sub>2</sub> (1pob) active site. Hesperidin molecule is shown in green colour. Hydrogen bonds are represented by green broken lines.

Pyrrolizidine alkaloids are secondary metabolites of several plant families for instance Boraginaceae or Asteraceae and are supposed to be toxic. The metabolic activation of pyrrolizidine alkaloids is catalyzed by hepatic cytochrome P450 and generates reactive pyrrolic metabolites that bind to cellular amino acids of proteins to form pyrrole-protein adducts leading to toxicity. This confirms the ability of pyrrolizidine alkaloids to bind the PLA<sub>2</sub> enzyme but the chronic use of pyrrolizidine alkaloids is very harmful [24,25]. PLA<sub>2</sub> catalyzes the rate-limiting step in the construction of pro-inflammatory eicosanoids and free radicals. The PLA<sub>2</sub> catalyzed reaction is considered to be

an important pathway for the production of reactive oxygen species (ROS) which in turn activates PLA<sub>2</sub> as well as lipid peroxidation and thereby substantially enhances chronic inflammatory diseases [26,27]. Hence, PLA<sub>2</sub> inhibition comes into consideration in the inhibition of inflammation. The antioxidants such as phenolic acid derivatives and flavonoids may also exhibit an important contribution in the interference of inflammatory reactions if they inhibit the phospholipase A<sub>2</sub> along with neutralizing free radical generation [28,29]. Our results are in agreement with the data reported by Dileep, *et al.* in which the inhibiting abilities of phenolic acid derivatives such as vanillic acid, gallic acid, syringic acid and protocatechuic acid against PLA<sub>2</sub> were reported [30].

### Fluorescence spectra of *Echium angustifolium* aqueous extract

One way to measure the degree and convenience of protein binding sites to small molecules is to use fluorescence quenching. Information relating to the number of binding sites, the binding constant  $K_a$ , and the distance between acceptors and donors can be willingly obtained using the Stern-Volmer kinetics and Forster's theory [31]. The fluorescence autograph of a protein is obtained from the aromatic residues. The fluorescence from the indole group in tryptophane (Trp) is tremendously sensitive to its environment and is a suitable spectroscopic probe for the structure and rotational dynamics surrounding the Trp residue [32,33]. The Trp residues in phospholipase A<sub>2</sub> can undergo electronic excitation in the visible region, and the emission can be quenched *via* particular mechanisms depending on the extent of "exposure" to the quencher. Therefore, changes in the intrinsic fluorescence and the bimolecular quenching rate constant of PLA<sub>2</sub> can be used to monitor structural changes in PLA<sub>2</sub> fluorescence and give information on Trp accessibility and how deep it is buried in the PLA<sub>2</sub> molecule. In PLA<sub>2</sub>, a Trp residue is buried in a hydrophobic fold [34]. The fluorescence spectrum shows a decrease of fluorescence intensity (Figure 2) of the snake venom after addition of 33  $\mu$ l of *Echium angustifolium* aqueous extract which could be related to a diversity of processes. It is well known that a decrease in fluorescence intensity can be caused by a range of molecular interactions such as molecular rearrangements, ground state complex formation, excited-state reactions, energy transfer or collisional quenching. The decrease in fluorescence emission intensity as shown in figure 2 was not escorted by a red or blue shift which may indicate that Trp residues buried in a hydrophobic environment have moved into a relatively polar environment consistent with earlier reports [35]. The decrease in fluorescence emission intensities rather indicate that binding of *Echium angustifolium* constituents may have talented a conformational change that moves Trp into a moderately more hydrophobic region. This explanation is in agreement with Gorbenko, *et al.* (2007) who found that the tryptophan fluorescence is quenched by interactions with polar ligands. Binding of proteins to lipid membranes decreases the access to these polar ligands and accordingly decreases the quenching effect [36]. In addition, quenching could be related to two more factors: first, the carboxylate of *Echium angustifolium* and amide moieties of PLA<sub>2</sub> must be in direct contact to bring about obvious quenching. The conjugation between the amide (or the keto) group and the carboxylate group leads to a lower  $\pi^*$  orbital, which is the lowest unoccupied molecular orbital (LUMO), able to accept an electron from the excited Trp. Second, since the constituents of *Echium angustifolium* have high electron density (hydrogen bonds with water molecules), which can be seen by molecular modeling. Their LUMO energies are strongly affected by water in aqueous solution. The obtained fluorescence results demonstrate how tryptophan fluorescence of PLA<sub>2</sub> become quenched in aqueous solution and is in agreements with the literature [35,37,38].

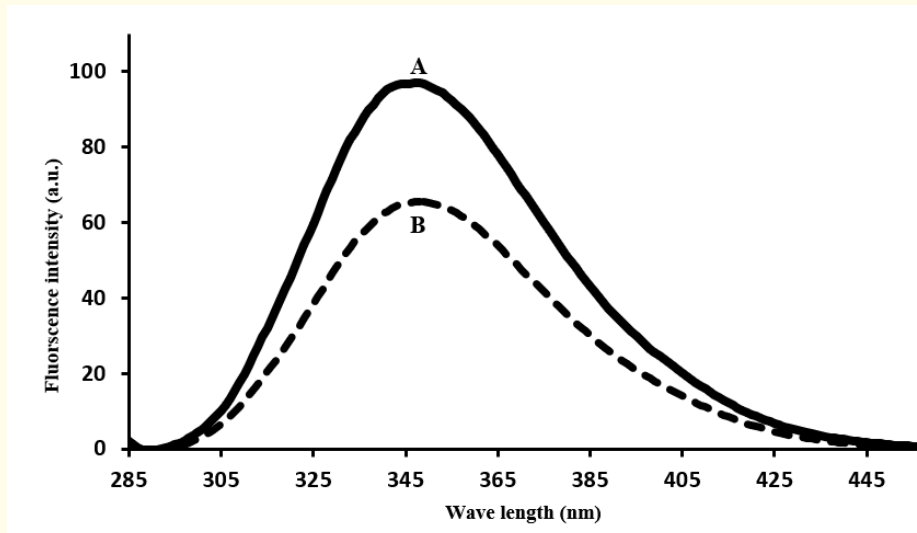


**Figure 2:** (A) Plot of fluorescence emission of snake venom (*Cerastes cerastes*) (24.6  $\mu$ g/ml) vs wavelength from 285 - 550 nm using excitation of  $\lambda$ 280 nm in 0.01M Tris, 0.1M NaCl at pH 7.4. (B) Fluorescence perturbation of snake venom by addition of 33  $\mu$ l (1.29g/30 ml) of *Echium angustifolium* aqueous extract. Spectra were corrected for background fluorescence contributions from the buffer solution and were scaled to visualize the change. The total volume in the cuvette was 2000  $\mu$ l.

### Calculation LD99 of *Cerastes cerastes* venom

Lethality data of *Cerastes cerastes* venom was calculated. The LD99 of *Cerastes cerastes* venom was 5 µg/kg as reported previously [39].

### Acute toxicity of *Cerastes cerastes* venom and its neutralization by *Echium angustifolium* aqueous extract and antivenom

The lethal dosage reflects the venom of the *Cerastes cerastes* snakes which are found in Libya is of high quality and very much strong in terms of its toxicity and lethality. *Cerastes cerastes* venom at a dose of 5 µg/kg (LD99) produced 100% mortality in mice. *Echium angustifolium* aqueous extract significantly increased mean survival time up to 13.0 ± 0.26 hours compared to 1.1 ± 0.1h before treatment. The protection fold could not protect animals from death when *Cerastes cerastes* venom was used alone. The *Echium angustifolium* aqueous extract when used at the dose of 2.0 ml (stock 1.29g/30 ml) solution was found to be more effective against *Cerastes cerastes* venom (13.0 hours) when compared with 8.5 hours using 0.5 ml (stock 1.29g/30 ml) solution. ASV [polyvalent anti-snake venom by Haffkine Bio-Pharmaceuticals Company (India)] was found to be more effective as compared with the *Echium angustifolium* aqueous extract showing a mean survival of two days for five mice and complete survival of one mouse and was consistent to our previously published work [40]. The pharmacological effects of *Cerastes cerastes* venoms could be classified into three main types, cytotoxic, hemotoxic [40-42] and neurotoxic. The main toxin related to these effects is PLA<sub>2</sub>, which is responsible for many pharmacological effects in snakebite victims. The PLA<sub>2</sub> is able to operate on pre- or post-synaptic junctions as antagonist of ion channels and muscarinic or nicotinic receptors to prevent or mitigate neurotoxicity such as paralysis and respiratory failure [42,43]. In addition, PLA<sub>2</sub> can cause local tissue damage resulting in swelling, blistering, bruising or necrosis. In addition, it has systemic effects eliciting hemostatic; hypovolemic shock and cardiovascular effects as coagulopathy, hemorrhage or hypotension and it is also reported to induce severe pain [44,45].

Because PLA<sub>2</sub> activity is a significant part of the venom toxicity, PLA<sub>2</sub> inhibitors are considered for testing drugs. Our results show that the aqueous extract of *Echium angustifolium* when given to the mice after they had received *Cerastes cerastes* at a dose 2.0 µl (stock 1.29g/30 ml) significantly increased mean survival time. This could be due to the interaction of venom components -mainly PLA<sub>2</sub> -with *Echium angustifolium* constituents which is in agreement with the result obtained by molecular docking. The result is in agreements with some previous studies in which some other botanical families such as *Fabaceae*, *Asteraceae*, *Apocynaceae*, *Lamiaceae*, *Rubiaceae*, *Euphorbiaceae*, *Araceae*, *Malvaceae* and *Acanthaceae* were found to be useful against snake bites [46,47]. Interestingly, some studies have reported that the crude extracts are already effective and may justify the growth and use of these herbal products.

However, despite of this potential application no natural antiophidic product is obtainable on the market. Literature concerning herbal products against snakebites is sparse [48].

### Conclusion

Our molecular docking and *in vivo* animal studies indicate that constituents of an aqueous plant extract from of *Echium angustifolium* are able to bind to active sites of PLA<sub>2</sub> causing inhibition of the enzyme which provides the bases for its substantial antiophidic activity against *Cerastes cerastes* venom.

### Bibliography

1. Appiah B. "Snakebite neglect rampant in Africa". *Canadian Medical Association Journal* 184 (2012): E27-E28.
2. Harrison RA, et al. "Preclinical antivenom-efficacy testing reveals potentially disturbing deficiencies of snakebite treatment capability in East Africa". *PLOS Neglected Tropical Diseases* (2017): 11.
3. Appiah B. "Snakebite neglect rampant in Africa". *Canadian Medical Association Journal* 184 (2012): E27-E28.

4. Mohamed AH., *et al.* "Toxic fractions of *Cerastes cerastes* venom". *Japanese Journal of Medical Science and Biology* 30 (1977): 205-207.
5. Siddiqi AR., *et al.* "Characterization of phospholipase A2 from the venom of Horned viper (*Cerastes cerastes*)". *FEBS Letters* 278 (1991): 14-16.
6. Gasanov SE., *et al.* "Phospholipase A2 and cobra venom cytotoxin Vc5 interactions and membrane structure". *General Physiology and Biophysics* 14 (1995): 107-123.
7. Alzahaby M., *et al.* "Some pharmacological studies on the effects of *Cerastes vipera* (Sahara sand viper) snake venom". *Toxicon* 33 (1995): 1299-1311.
8. Cavalcante WLG., *et al.* "Neuromuscular paralysis by the basic phospholipase A2 subunit of crotoxin from *Crotalus durissus terrificus* snake venom needs its acid chaperone to concurrently inhibit acetylcholine release and produce muscle blockage". *Toxicology and Applied Pharmacology* 334 (2017): 8-17.
9. Mohamed AH., *et al.* "Toxic fractions of *Cerastes cerastes* venom". *Japanese Journal of Medical Science and Biology* 30 (1977): 205-207.
10. Rigoni M., *et al.* "Snake phospholipase A2 neurotoxins enter neurons, bind specifically to mitochondria, and open their transition pores". *Journal of Biological Chemistry* 283 (2008): 34013-34020.
11. Vulfius CA., *et al.* "Pancreatic and snake venom presynaptically active phospholipases A2 inhibit nicotinic acetylcholine receptors". *PLoS One* 12 (2017): e0186206.
12. Hamza M., *et al.* "Cost-Effectiveness of Antivenoms for Snakebite Envenoming in 16 Countries in West Africa". *PLOS Neglected Tropical Diseases* 10 (2016): e0004568.
13. Ahmed SM., *et al.* "Emergency treatment of a snake bite: Pearls from literature". *Journal of Emergencies, Trauma, and Shock* 1 (2008): 97-105.
14. Mor-Mussery A., *et al.* "New methodology for quantifying the effects of perennials on their patch productivity in semi-arid environments". *Environmental Management* 55 (2015): 1139-1146.
15. El Rokh AR., *et al.* "Sucrose diester of aryldihydronaphthalene-type lignans from *Echium angustifolium* Mill. and their antitumor activity". *Phytochemistry* 149 (2018): 155-160.
16. Silver KS., *et al.* "Voltage-Gated Sodium Channels as Insecticide Targets". *Advances in Insect Physiology* 46 (2014): 389-433.
17. Dong K., *et al.* "Molecular Biology of Insect Sodium Channels and Pyrethroid Resistance". *Insect Biochemistry and Molecular Biology* 50 (2014): 1-17.
18. Tiwari R., *et al.* "Carborane clusters in computational drug design: a comparative docking evaluation using AutoDock, FlexX, Glide, and Surflex". *Journal of Chemical Information and Modeling* 49 (2009): 1581-1589.
19. Markwell MA., *et al.* "A modification of the Lowry procedure to simplify protein determination in membrane and lipoprotein samples". *Analytical Biochemistry* 87 (1978): 206-210.
20. Holt PA., *et al.* "Molecular docking of intercalators and groove-binders to nucleic acids using Autodock and Surflex". *Journal of Chemical Information and Modeling* 48 (2008): 1602-1615.
21. Gilad Y and Senderowitz H. "Docking studies on DNA intercalators". *Journal of Chemical Information and Modeling* 54 (2014): 96-107.
22. Scott DL., *et al.* "Interfacial catalysis: the mechanism of phospholipase A2". *Science* 250 (1990): 1541-1546.

23. White SP, *et al.* "Crystal structure of cobra-venom phospholipase A2 in a complex with a transition-state analogue". *Science* 250 (1990): 1560-1563.
24. Kubitza C., *et al.* "Crystal structure of pyrrolizidine alkaloid N-oxygenase from the grasshopper *Zonocerus variegatus*". *Acta Crystallographica Section F: Structural Biology* 74 (2018): 422-432.
25. Ma J., *et al.* "Pyrrole-protein adducts - A biomarker of pyrrolizidine alkaloid-induced hepatotoxicity". *Journal of Food and Drug Analysis* 26 (2018): 965-972.
26. Suladze S., *et al.* "Pressure Modulation of the Enzymatic Activity of Phospholipase A2, A Putative Membrane-Associated Pressure Sensor". *Journal of the American Chemical Society* 137 (2015): 12588-12596.
27. Godkin JD., *et al.* "Phospholipase A2 regulation of bovine endometrial (BEND) cell prostaglandin production". *Reproductive Biology and Endocrinology* 6 (2008): 44.
28. Gelb MH., *et al.* "Inhibition of phospholipase A2". *The FASEB Journal* 8 (1994): 916-924.
29. Lombardo D and Dennis EA. "Cobra venom phospholipase A2 inhibition by manoalide. A novel type of phospholipase inhibitor". *Journal of Biological Chemistry* 260 (1985): 7234-7240.
30. Dileep KV., *et al.* "Comparative studies on the inhibitory activities of selected benzoic acid derivatives against secretory phospholipase A2, a key enzyme involved in the inflammatory pathway". *Molecular Omics* 11 (2015): 1973-1979.
31. Yang Y., *et al.* "Binding research on flavones as ligands of beta-amyloid aggregates by fluorescence and their 3D-QSAR, docking studies". *Journal of Molecular Graphics and Modelling* 29 (2010): 538-545.
32. Sumandea M., *et al.* "Roles of aromatic residues in high interfacial activity of *Naja naja atra* phospholipase A2". *Biochemistry* 38 (1999): 16290-16297.
33. Kuipers OP., *et al.* "Insight into the conformational dynamics of specific regions of porcine pancreatic phospholipase A2 from a time-resolved fluorescence study of a genetically inserted single tryptophan residue". *Biochemistry* 30 (1991): 8771-8785.
34. Yang CC and Chang LS. "Assessment of the role of tryptophan residues in phospholipase A2 by fluorescence quenching". *International Journal of Biological Macromolecules* 11 (1989): 13-16.
35. Kenoth R., *et al.* "Structural determination and tryptophan fluorescence of heterokaryon incompatibility C2 protein (HET-C2), a fungal glycolipid transfer protein (GLTP), provide novel insights into glycolipid specificity and membrane interaction by the GLTP fold". *Journal of Biological Chemistry* 285 (2010): 13066-13078.
36. Gorbenko GP., *et al.* "Binding of lysozyme to phospholipid bilayers: evidence for protein aggregation upon membrane association". *Biophysical Journal* 93 (2007): 140-153.
37. Gong AQ and Zhu XS. "Determination of epristeride by its quenching effect on the fluorescence of L-tryptophan". *Journal of Pharmaceutical Analysis* 3 (2013): 415-420.
38. Peng HL and Callender R. "Mechanism for Fluorescence Quenching of Tryptophan by Oxamate and Pyruvate: Conjugation and Solvation-Induced Photoinduced Electron Transfer". *The Journal of Physical Chemistry B* 122 (2018): 6483-6490.
39. Enas A Sadawe., *et al.* "Olea Europaea Leaves Delay the Onset of Toxicity of *Cerastes cerastes* Venom in Albino Mice". *Journal of Pharmaceutical Research* 4 (2019): 1-3.
40. Valenta J., *et al.* "Analysis of hemocoagulation tests for prediction of venom-induced consumption coagulopathy development after Viperidae bite". *Bratislavske Lekarske Listy* 120 (2019): 566-568.

41. Crofts SB., *et al.* "How do morphological sharpness measures relate to puncture performance in viperid snake fangs?" *Biology Letters* 15 (2019): 20180905.
42. Esiene A., *et al.* "Severe Viperidae envenomation complicated by a state of shock, acute kidney injury, and gangrene presenting late at the emergency department: a case report". *BMC Emergency Medicine* 19 (2019): 26.
43. Abdel-Aty AM., *et al.* "A hemorrhagic metalloprotease of Egyptian *Cerastes vipera* venom: Biochemical and immunological properties". *International Journal of Biological Macromolecules* 130 (2019): 695-704.
44. Bittencourt GB., *et al.* "Photoreceptors morphology and genetics of the visual pigments of *Bothrops jararaca* and *Crotalus durissus terrificus* (Serpentes, Viperidae)". *Vision Research* 158 (2019): 72-77.
45. Ozverel CS., *et al.* "Investigating the cytotoxic effects of the venom proteome of two species of the Viperidae family (*Cerastes cerastes* and *Cryptelytrops purpureomaculatus*) from various habitats. Comp Biochem". *Physiology Part C Toxicology and Pharmacology* 220 (2019): 20-30.
46. Gomes A., *et al.* "Herbs and herbal constituents active against snake bite". *Indian Journal of Experimental Biology* 48 (2010): 865-878.
47. Penchalapratap G., *et al.* "Herbal remedies for Snake bites in Ethnic practices of Chittoor District, Andhra Pradesh". *Ancient Science of Life* 29 (2010): 13-16.
48. Gupta YK and Peshin SS. "Do herbal medicines have potential for managing snake bite envenomation?" *Toxicology International* 19 (2012): 89-99.

**Volume 4 Issue 10 October 2020**

**© All rights reserved by Abdul M Gbaj., *et al.***